Passively mode-locked 2.7 and 3.2 μm GaSb-based cascade diode lasers.

T. Feng, L. Shterengas, T. Hosoda, G. Kipshidze, *Member, IEEE*, A. Belyanin, C.C. Teng, J. Westberg, G. Wysocki, and G. Belenky, *Fellow, IEEE*.

Abstract—The passively mode-locked type-I quantum well cascade diode lasers operating near 2.7 and 3.2 µm generated trains of the ~10 ps long pulses with average power up to 10 mW. The devices based on laser heterostructures with reinforced carrier confinement required increased reverse bias voltages applied to absorber sections to operate in mode-locked regime. The autocorrelation measurements showed that lasers generated strongly chirped pulses with temporal width an order of magnitude above transform limit. The application of the external feedback led to narrowing of the laser emission spectra accompanied by an order of magnitude reduction of the intermodal beat note linewidth. The multiheterodyne beat notes have been observed for devices stabilized by external feedback.

Index Terms—mode-locked lasers, semiconductor lasers, GaSb, optical frequency comb, quantum wells, cascade lasers.

I. INTRODUCTION

HE stable trains of ultrashort light pulses with wide frequency comb spectrum generated by mode-locked lasers are key elements for many important applications such as nonlinear frequency conversion, laser radars, dual-comb spectroscopy, etc. Interband semiconductor lasers with gain media carrier lifetime of the order of ns can be passively modelocked (PML) with a saturable absorber made of a reverse biased section of the laser waveguide. This split-contact architecture has been proven to be very effective and corresponding interband non-cascade passively mode-locked diode lasers operating in spectral region below 2.2 µm have been demonstrated [1-5]. The need to extend the wavelength range of the semiconductor optical frequency comb sources for multi-heterodyne spectroscopy initiated the on-going efforts to passively mode-lock the interband cascade lasers utilizing type-II quantum well (QW) active regions and operating in spectral region from about 3.2 to 3.7 µm [6]. At longer wavelengths, the quantum cascade lasers demonstrated the optical frequency comb operation in the frequency-modulated regime when the cavity dispersion was compensated [7,8]. In year 2018 our research team reported on design, fabrication characterization of the 3.25 µm passively-mode-locked GaSbbased type-I QW cascade diode lasers [9]. The lasers emitted

The work was supported in part by US Army Research Office, grant W911NF-18-1-0057 and US National Science Foundation, grant ECCS-1707317

T. Feng, L. Shterengas, T. Hosoda1, G. Kipshidze, G. Belenky are with State University of New York at Stony Brook, Stony Brook, NY 11794, USA (e-mail: leon.shterengas@stonybrook.edu).

train of the strongly chirped pulses with substantial jitter, presumably, caused by spontaneous emission. The spontaneous emission noise can explain the intermodal beat note Lorentzian linewidth of about 200 kHz observed in these devices. The multiheterodyne spectroscopy requires highly coherent frequency comb emitters. The devices reported in [9] did not possess required coherence and we were not able to resolve multiheterodyne beatnotes using free-running devices.

In order to improve the device coherence here we tested an optical feedback scheme [10,11] that led to narrowing of the intermodal beat note by over an order of magnitude (compare Figures 1a and 1b). The devices reported in [9] with internal RF linewidth ~300 kHz were used for the demonstration.

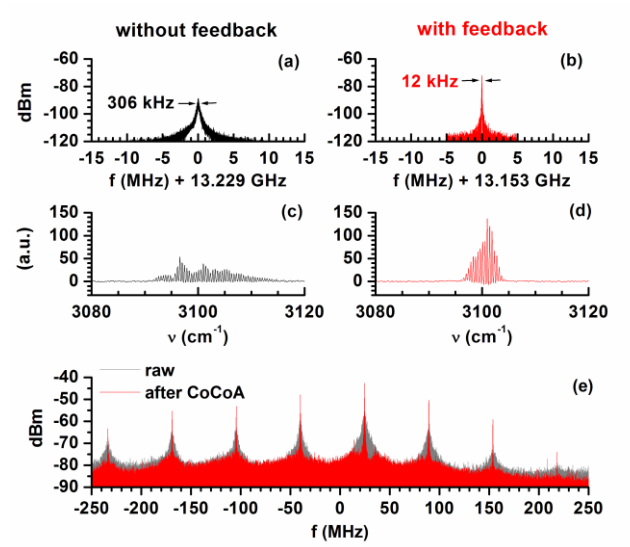


Figure 1. (a) Intermodal beat note linewidth of 306 kHz is measured for a free running device [9]. (b) Under proper optical feedback, the intermodal beat note linewidth can be reduced to 12 kHz for the same device under the same bias conditions. The (c) and (d) The corresponding FTIR optical spectra. (e) Multiheterodyne spectrum from a pair of lasers (both under optical feedback stabilization). After applying computational correction to address fluctuations in the carrier frequency and repetition rate, the improved multiheterodyne spectrum is obtained as shown in the same figure for comparison.

The detuning of the external reflector from its optimal position led to gradual increase of the beat note linewidth accompanied by also gradual broadening of the laser emission spectrum. This effect suggests that an important mechanism

A. Belyanin is with Texas A&M University, College Station, TX 77843, USA. C.C. Teng, J. Westberg, G. Wysocki are with Princeton University, Princeton, NJ 08544, USA.

that helps to improve mode coherence is related to suppression of modes at the edges of the gain curve which are weaker and most likely are less coherent (e.g. due to impact of group velocity dispersion). As a result, reduced spectral coverage is observed (compare Figures 1c and 1d) in case of more coherent operation with narrowed intermodal beat note. The two lasers are then aligned to beat with each other on a fast photodetector (Vigo System S.A.), and the corresponding raw RF multiheterodyne spectrum is shown in Figure 1e. In this measurement, the repetition rate difference between the two lasers is 65 MHz, which corresponds to the spacing between the multiheterodyne beat notes. For frequency combs, the carrier frequency and repetition rate fluctuations can be corrected using computational algorithms [12-14] due to highly correlated noise in its optical spectrum, and for highly coherent comb sources the Fourier-limited multiheterodyne beat notes are usually obtained after correction. We applied computational coherent averaging (CoCoA) to the acquired multiheterodyne spectrum, and the corrected results are plotted also in Figure 1e. We observe reduced noise pedestal after CoCoA indicating some but still limited degree of coherence amongst the optical modes.

In this work we demonstrate the mode-locked operation of the cascade diode lasers in extended spectral range and with improved power and noise characteristics. The 2.7 μm passively mode-locked lasers demonstrated intermodal beat note linewidths down to 30 kHz and average output power up to 10 mW – an order of magnitude improvement compared to devices in [9]. Arguably, the improvement of the noise characteristics of the pulse train generated by PML laser was associated with reduced coupling of the spontaneous emission to the laser mode in emitters with reduced QW optical confinement. It was shown that enhancement of the carrier confinement barriers improved the laser efficiency but led to the higher operating voltages of the saturable absorber section.

II. HETEROSTRUCTURE DESIGN AND DEVICE FABRICATION

Figure 2 illustrates the difference between the laser heterostructures used in this work (Figures 2b and 2c) and the reference one (Figure 2a) reported in [9]. The quinary alloy layer between p-cladding and active region was replaced with GaSb binary. The lasers emitting near 3.2 µm used 350 nm thick GaSb layer while those emitting near 2.7 µm had 500 nm thick ones. The widened high index GaSb layer in the latter led to reduced optical mode coupling with QWs. In order to preserve the hole confinement in the active OW adjacent to the GaSb layer we introduced one additional graded composition AlGaAsSb layer. In laser heterostructure designed to emit near 3.2 µm we utilized graded composition layers with initial aluminum content of 80 % (50% was used in devices studied in reference [9]). The increased aluminum composition led to enhancement of the hole confinement in active OWs by more than 100 meV as can be estimated following [15,16]. The devices operating near 2.7 µm utilized graded composition layers with initial aluminum content of 50% which still ensured strong hole confinement thanks to a shift of the top of the valence band in QWs providing optical gain near 2.7 µm. Figure 1 shows that the use of the GaSb layer instead of quinary AlGaInAsSb leads to substantial increase (by 200 – 300 meV)

of the band discontinuity between p-cladding and separate confinement layer.

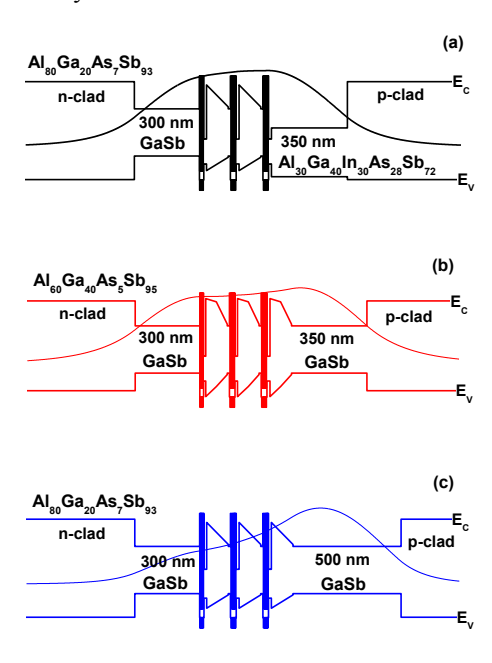


Figure 2. The band diagrams of the reference 3.25 μm (a), modified 3.2 μm (b), and modified 2.7 μm (c) emitting laser heterostructures. The corresponding calculated transverse modal intensity distributions are superimposed on the band diagrams.

Figure 3 illustrates the fabricated lasers and shows details of the etching profile in the corresponding scanning electron microscope images. The ridges were etched through p-cladding down to the middle of the waveguide core to ensure strong current confinement in cascade lasers prone to lateral current spreading. The 20 μ m wide and ~2 μ m deep gap was etched between amplifier and absorber section of the devices to minimize electrical crosstalk.

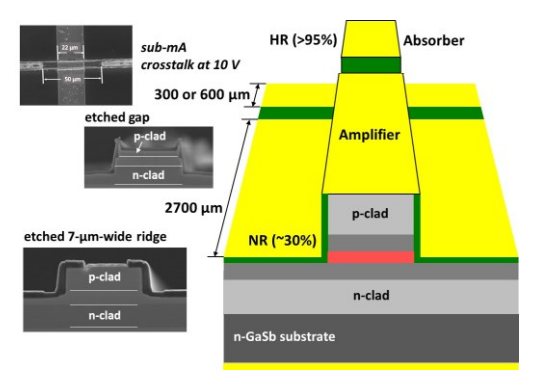


Figure 3. The split contact ridge waveguide passively mode-locked laser design with 2.7 mm long amplifier section and 300 or 600 μm long absorber sections. The scanning electron microscope images shown on the left illustrate: top view of the 20 μm wide etched gap between absorber and amplifier sections (top), cross section view of the etching profile in the isolation gap (middle), and etching profile of the narrow ridge waveguide in the amplifier and absorber sections (bottom).

The processed laser wafers were cleaved into individual devices with 2.7 mm long amplifier sections and 300 or 600 μm long absorber sections. The laser facets were coated neutral/high-reflection (NR/HR, $\sim\!\!30/95\%$) on amplifier and absorber sides, respectively. The electrical isolation between amplifier

and absorber sections was confirmed by measuring sub-mA current flowing between these sections when negative 10 V bias was applied to absorber with respect to amplifier.

III. CHARACTERIZATION RESULTS AND DISCUSSION

Figure 4 plots the light-current-voltage characteristics measured for 2.7 and 3.2 μm emitting lasers with absorber section lengths of 300 μm . When both amplifier and absorber were forward biased the devices generated above 20 mW of CW output power from NR coated facet. The output power and threshold current of the Fabry-Perot 3.2 μm emitting devices based on the heterostructure with enhanced hole confinement (Figure 1) were improved nearly twofold compared to devices reported in [9]. The 2.7 μm Fabry-Perot lasers show higher threshold than 3.2 μm devices presumably due to reduced optical confinement of active QWs (Figure 2).

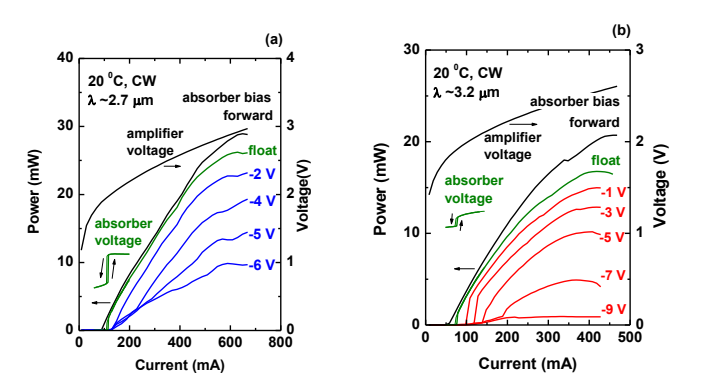


Figure 4. The power-current-voltage characteristics measured for 2.7 μm (a) and 3.2 μm (b) lasers at 20 ^{o}C in CW regime at different absorber section bias conditions. The devices have the amplifier section length of 2.7 mm and absorber section of 300 μm . The curves marked "absorber voltage" show the voltage measured at absorber terminal when it was left floating. The floating absorber power-current and voltage-current dependences are shown for increasing and decreasing currents measurement conditions. The other curves are measured under increasing current condition.

When the absorber section was left floating and only the amplifier section was forward-biased the devices demonstrated characteristic hysteresis in light-current curves. The measured potential of the floating absorber demonstrates abrupt voltage change at threshold (also with hysteresis) associated with appearance of the large number of photons in the cavity. The application of the reverse bias to the absorber section led to monotonic reduction of the average output power caused by decrease of the absorber recovery time. Once the absorber QWs recovery time is reduced sufficiently by field assisted thermionic emission the devices can operate in self-starting mode-locked regime. The reverse biased absorber operates as an in-situ ultra-fast photodetector and the radio-frequency (RF) component of the absorber voltage was used to measure the intermodal beat note spectra. Figures 5a and 5b show the current-frequency maps of the strong intermodal beat notes for 2.7 µm lasers at the absorber bias of -6 V, and for 3.2 µm lasers at the absorber bias of -9 V. Only weak and unstable RF beats were observed at absorber biases of -4 and -5 V for 2.7 µm emitters and at -7 and -8 V for 3.2 µm ones. At lower biases the RF spectra showed no beat notes. It can be speculated that a higher QW hole confinement barrier that improved the Fabry-Perot laser performance requires higher voltages to extract

photoexcited carriers from absorber QWs. Figures 5c and 5d plot the spectra of the RF beat note at the amplifier currents of 280 and 350 mA and absorber biases of -6 and -9 V for 2.7 and 3.2 μ m emitters, respectively. The RF spectra were well fitted by Lorentzian curves with linewidth of about 30 kHz and 100 kHz for 2.7 and 3.2 μ m lasers. The peak frequencies correspond well to cavity roundtrip times with modal effective group indexes in the range from 3.8 to 3.9. The RF linewidths in the range of tens of kHz indicate contribution of the spontaneous emission noise to the laser modes [17].

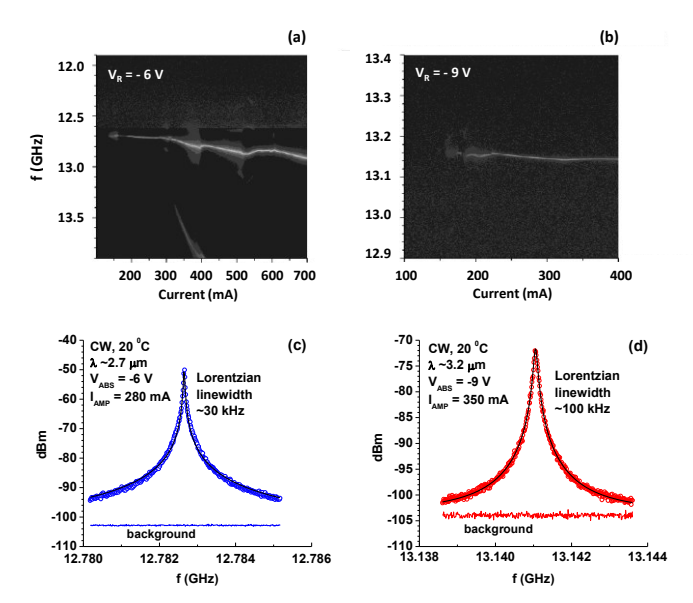


Figure 5. The RF intensity maps (in dB scale) taken over amplifier section current range from 100 to 700 mA and for -6 V of absorber section bias for 2.7 μm laser (a); and from 100 to 400 mA and for -9 V of absorber section bias for 3.2 μm laser (b). The figures (c) and (d) show the high-resolution intermodal beat notes measured at the bias conditions of amplifier section currents of 280 mA and absorber section bias of -6 V for 2.7 μm , and at 350 mA of current and -9 V bias for 3.2 μm lasers, respectively. Lorentzian fits and noise floors are also shown.

Figures 6a and 6b show the laser spectra measured at different amplifier section currents and at -6 (no RF beat note observed at any amplifier section current) and -9 V (strong RF beat note observed at amplifier section currents above ~200 mA) of absorber section bias voltages for 3.2 µm emitters, respectively. The periodic modulations of the laser emission spectra apparent in both mode-locked and CW regimes are caused by parasitic 300-um-long Fabry-Perot etalon introduced into the cavity by deep etching of the gap between absorber and amplifier sections. The spectra of the 3.2 µm emitting device operating at absorber bias voltage of -9 V tend to change their shape qualitatively once the amplifier section current goes above 200 mA. This change correlates well with the formation of a strong RF beat note (Figure 5a). Figure 6 shows that the laser emission bandwidth does not become wider in the modelocking regime. However, the envelope of the laser emission spectra tends to acquire the smoothed shape corresponding to the pulse formation. At the top of the Figures 6a and 6b there shown the 2-photon interferometric autocorrelation (IAC) scans measured at 350 mA of amplifier current and -6 and -9 V absorber bias voltages, respectively. The IAC measured at the absorber section bias of -6 V does not indicate the pulsed operation. When the device absorber section is biased at -9 V

one can observe a strong RF beat note, output spectrum modification, and IAC indicating the presence of the ~12 ps wide chirped pulses. We measured autocorrelation over a wide range of delays with limited resolution (essentially, close to intensity autocorrelation regime) in order to be able to estimate the width of the chirped pulses (IAC measurements were performed with steps of about 33 fs which was insufficient to resolve the fringes near the zero delay corresponding to ~3 ps coherence region). The spectral chirp in the pulse leads to pedestal in IAC surrounding the coherence region. The uncompensated cavity dispersion accounts for the formation of the chirped pulse. The pedestal corresponding to the intensity autocorrelation shows expected peak to background intensity ratio approaching 3 to 1. Thus estimated ~12 ps pulse width corresponds to about an order of magnitude above the transform limit for the observed laser emission spectrum bandwidth of ~10 nm. One can conclude that cavity dispersion and self-phase modulation are the critical factors limiting the ability of the saturable absorber to phase lock all longitudinal modes in ~10 nm wide spectrum and form an optical frequency comb within the laser emission bandwidth. The increase of the absorber section width from 300 to 600 µm had an adverse effect on 3.2 µm device operation, i.e. the lasers did not show any power for the absorber section reverse bias below 0 V.

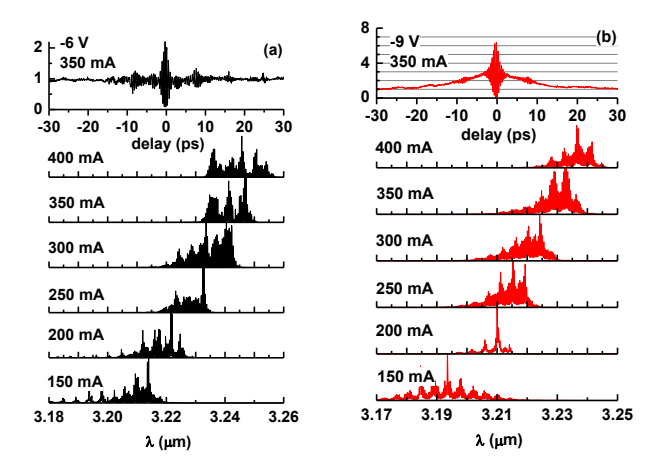


Figure 6. The laser emission spectra (linear scale) measured at different amplifier section currents varied from 150 to 400 mA, and absorber bias voltages of -6 V (a) and -9 V (b) for 3.2 μm emitters. The IAC scans measured at 350 mA of amplifier section current at corresponding absorber section biases are shown on top.

Figure 7 shows the laser emission spectra measured for 2.7 µm laser under the bias corresponding to the presence of a strong RF beat note. The laser emission spectra demonstrate the bandwidth of about 20 nm at amplifier current of 280 mA. Once the current is increased up to 300 mA the laser spectrum broadens significantly and tends to split into two bands with further current increase. This phenomenon was observed in the first generation of the GaSb-based cascade diode lasers but only when they were operating in CW, i.e. not in the mode-locked regime [9]. The similarity to the coherent multimode instability observed in mid-infrared QCLs [18] was pointed out. In the 2.7 µm lasers studied in this work the spectral splitting can be seen in a certain range of the currents (from ~300 to ~400 mA) even with reverse biased absorber and apparent RF beat. The spectral splitting correlate with appearance of the additional

lower frequency branch in RF spectrum (fig. 5a). The IAC studies confirm the mode-locked chirped pulse laser operation with the pulse width an order of magnitude above the transform limit, similarly to the case of 3.2 μm emitters. The peak-to-background contrast of an IAC scan (Figure 6) was limited due to certain misalignment between branches of the Michelson interferometer (alignment of the Michelson interferometer for 2.7 μm emitters was additionally complicated by the absence of an infrared camera sensitive in this spectral region in our lab). The 2.7 μm emitters with a 600 μm long absorber section operated well when a reverse bias was applied to an absorber but generated somewhat reduced output power levels. The measurement of the RF spectra of the devices with increased absorber section length did not reveal any improvement in terms of the stability of the mode-locking regime.

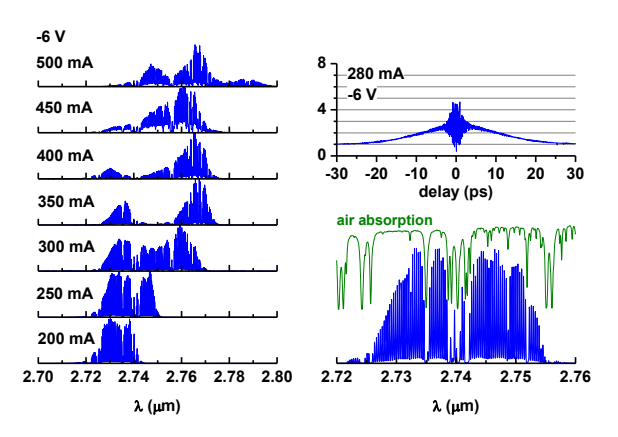


Figure 7. The 2.7 μ m laser emission spectra measured at different amplifier section currents varied from 150 to 500 mA and at absorber bias voltage of -6 V. The right panel shows the IAC (top) scans measured at 280 mA of amplifier section current and -6 V of absorber section voltage, and corresponding laser emission spectrum overlapped with room air transmission spectrum showing atmospheric absorption lines associated with water vapor.

IV. CONCLUSION

The split-contact passively mode-locked GaSb-based type-I QW cascade diode laser operating near 2.7 and 3.2 µm have been designed, fabricated and characterized. The devices utilizing laser heterostructures with improved hole confinement demonstrated improved laser parameters but required higher reverse bias voltages applied to absorber sections to operate in a stable mode-locked regime. The lasers generated 10 - 15 ps strongly chirped pulses at repetition frequencies about 13 GHz and average power up to 10 mW. The intermodal beat notes of 2.7 µm emitters had the Lorentzian linewidth of about 30 kHz. The laser emission spectral bandwidth was up to 20 nm. The order of magnitude reduction of the intermodal beat note linewidth was demonstrated in devices with external feedback. The multiheterodyne beat notes have been observed between two passively-mode locked lasers stabilized by external feedback. The compensation of the cavity dispersion is required to achieve generation of the wide bandwidth optical frequency combs by type-I QW PML cascade diode lasers.

REFERENCES

[1]. K. Merghem, R. Teissier, G. Aubin, A. M. Monakhov, A. Ramdane,

- A.N. Baranov, "Passive mode locking of a GaSb-based quantum well diode laser emitting at 2.1 μ m", Appl. Phys. Lett. 107, 111109 (2015);
- [2]. X. Li, H. Wang, Z. Qiao, X. Guo, G. I. Ng, Y. Zhang, Z. Niu, C. Tong, C. Liu, "Modal gain characteristics of a 2 μm InGaSb/AlGaAsSb passively mode-locked quantum well laser", App. Phys. Lett. 111, 251105 (2017);
- [3]. Liu, Z. Lu, S. Raymond, P. J. Poole, P. J. Barrios, and D. Poitras, "Dual-wavelength 92.5 GHz self-mode-locked InP-based quantum dot laser," Opt. Lett. 2008, 33 (15), 1702-1704.
- [4]. H. Xiaodong, A. Stintz, L. Hua, A. Rice, G.T. Liu, L.P. Lester, J. Cheng, M.J. Malloy, "Bistable operation of a two-section 1.3 μm InAs quantum dot laser-absorption saturation and the quantum confined Stark effect," IEEE J. Quantum Electron. 2001, 37, 414.
- [5]. A. Pimenov, T. Habruseva, D. Rachinskii, S.P. Hegarty, G. Huyet, A.G. Vladimirov, "Effect of dynamical instability on timing jitter in passively mode-locked quantum-dot lasers", Opt. Lett. 2014, 39, 24.
- [6]. M. Bagheri, C. Frez, L.A. Sterczewski, I. Gruidin, M. Fradet, I. Vurgaftman, C.L. Canedy, W.W. Bewley, C.D. Merritt, C.S. Kim, M. Kim, J.R. Meyer, "Passively mode-locked interband cascade optical frequency combs", Nat. Sci. Rep. 8, 3322 (2018);
- [7]. A. Hugi, G. Villares, S. Blaser, H. Liu, and J. Faist, "Mid-infrared frequency comb based on a quantum cascade laser," Nature 492, 229 (2012):
- [8]. D. Kazakov, M. Piccardo, Y. Wang, P. Chevalier, T. S. Mansuripur, Chung-En Zah, K. Lascola, A. Belyanin, F. Capasso, "Self-starting harmonic frequency comb generation in a quantum cascade laser", Nature Photon 11, 789 (2017);
- [9]. T. Feng, L. Shterengas, T. Hosoda, A. Belyanin, G. Kipshidze, "Passive Mode-Locking of 3.25 μm GaSb-Based Cascade Diode Lasers", ACS Photon. 5, 4978 (2018).
- [10]. O. Solgaard, K.Y. Lau, "Optical feedback stabilization of the intensity oscillations in ultrahigh-frequency passively mode-locked monolithic quantum-well lasers", IEEE Photon. Technol. Lett. 5, 1264 (1993).
- [11]. C. Teng, J. Westberg, and G. Wysocki, "Optical-feedback-stabilized quantum cascade laser frequency combs," in Conference on Lasers and Electro-Optics (OSA, 2019), p. STu4N.3.
- [12]. D. Burghoff, Y. Yang, and Q. Hu, "Computational multiheterodyne spectroscopy," Sci. Adv. 2, e1601227 (2016).
- [13]. N. B. Hébert, J. Genest, J.-D. Deschênes, H. Bergeron, G. Y. Chen, C. Khurmi, D.G. Lancaster, "Self-corrected chip-based dual-comb spectrometer," Opt. Express 25, 8168 (2017).
- [14]. L.A. Sterczewski, J. Westberg, and G. Wysocki, "Computational coherent averaging for free-running dual-comb spectroscopy," arXiv:1805. 11146 (2018).
- [15]. I. Vurgaftman, J.R. Meyer, and L.R. Ram-Mohan, "Band parameters for III-V compound semiconductors and their alloys", J. Appl. Phys. 89, 5815 (2001):
- [16]. G.P. Donati, R. Kaspi, and K.J. Malloy, "Interpolating semiconductor alloy parameters: Application to quaternary III-V band gaps", J. Appl. Phys. 94, 5814 (2003).
- [17]. K. Hsu, C.M. Verber, R. Roy, "Stochastic mode-locking theory for external-cavity semiconductor lasers," J. Opt. Soc. Amer. B 8, 262 (1991).
- [18]. A. Gordon, C. Y. Wang, L. Diehl, F. X. Kärtner, A. Belyanin, D. Bour, S. Corzine, G. Höfler, H. C. Liu, H. Schneider, T. Maier, M. Troccoli, J. Faist, F. Capasso, "Multimode regimes in quantum cascade lasers: From coherent instabilities to spatial hole burning", Phys. Rev. A 2008, 77, 053804.